AMERICAN SOCIETY FOR MICROBIOLOGY | mBio®

RESEARCH ARTICLE
Host-Microbe Biology

Serine-Arginine Protein Kinase 1 Regulates Ebola Virus Transcription

Yuki Takamatsu,[a,d] Verena Krähling,[a,b] Larissa Kolesnikova,[a] Sandro Halwe,[a,b] Clemens Lier,[a] Stefan Baumeister,[c] Takeshi Noda,[d] Nadine Biedenkopf,[a,b] Stephan Becker[a,b]

[a]Institut für Virologie, Philipps-Universität Marburg, Marburg, Germany
[b]German Center of Infection Research (DZIF), Partner Site Giessen-Marburg-Langen, Marburg, Germany
[c]Protein Analytics, Faculty of Biology, Philipps University Marburg, Marburg, Germany
[d]Laboratory of Ultrastructural Virology, Institute for Frontier Life and Medical Sciences, Kyoto University, Kyoto, Japan

ABSTRACT Ebola virus (EBOV) causes a severe and often fatal disease for which no approved vaccines or antivirals are currently available. EBOV VP30 has been described as a viral phosphoprotein, and nonphosphorylated VP30 is essential and sufficient to support secondary transcription in an EBOV-specific minigenome system; however, phosphorylatable serine residues near the N terminus of VP30 are required to support primary viral transcription as well as the reinitiation of VP30-mediated transcription at internal EBOV genes. While the dephosphorylation of VP30 by the cellular phosphatase PP2A was found to be mediated by nucleoprotein, the VP30-specific kinases and the role of phosphorylation remain unknown. Here, we report that serine-arginine protein kinase 1 (SRPK1) and SRPK2 phosphorylate serine 29 of VP30, which is located in an N-terminal $R_{26}xxS_{29}$ motif. Interaction with VP30 via the $R_{26}xxS_{29}$ motif recruits SRPK1 into EBOV-induced inclusion bodies, the sites of viral RNA synthesis, and an inhibitor of SRPK1/SRPK2 downregulates primary viral transcription. When the SRPK1 recognition motif of VP30 was mutated in a recombinant EBOV, virus replication was severely impaired. It is presumed that the interplay between SRPK1 and PP2A in the EBOV inclusions provides a comprehensive regulatory circuit to ensure the activity of VP30 in EBOV transcription. Thus, the identification of SRPK1 is an important mosaic stone that completes our picture of the players involved in Ebola virus transcription regulation.

IMPORTANCE The largest Ebola virus (EBOV) epidemic in West Africa ever caused more than 28,000 cases and 11,000 deaths, and the current EBOV epidemic in the Democratic Republic of the Congo continues, with more than 3,000 cases to date. Therefore, it is essential to develop antivirals against EBOV. Recently, an inhibitor of the cellular phosphatase PP2A-mediated dephosphorylation of the EBOV transcription factor VP30 has been shown to suppress the spread of Ebola virus. Here, we identified the protein kinase SRPK1 as a VP30-specific kinase that phosphorylates serine 29, the same residue that is dephosphorylated by PP2A. SRPK1-mediated phosphorylation of serine 29 enabled primary viral transcription. Mutation of the SRPK1 recognition motif in VP30 resulted in significant growth inhibition of EBOV. Similarly, elevation of the phosphorylation status of serine 29 by overexpression of SRPK1 inhibited EBOV growth, highlighting the importance of reversible phosphorylation of VP30 as a potential therapeutic target.

KEYWORDS VP30, Ebola virus, kinase, protein phosphorylation, transcription

Reversible phosphorylation is an important posttranslational process that regulates protein conformation, thereby promoting protein-protein interactions and signal transduction and regulating protein synthesis and degradation (1–3). Similarly, for

Citation Takamatsu Y, Krähling V, Kolesnikova L, Halwe S, Lier C, Baumeister S, Noda T, Biedenkopf N, Becker S. 2020. Serine-arginine protein kinase 1 regulates Ebola virus transcription. mBio 11:e02565-19. https://doi.org/10.1128/mBio.02565-19.

Invited Editor Sean P. J. Whelan, Harvard Medical School

Editor Diane E. Griffin, Johns Hopkins Bloomberg School of Public Health

Address correspondence to Stephan Becker, Becker@staff.uni-marburg.de.

Received 27 September 2019
Accepted 13 January 2020
Published 25 February 2020

many important human RNA viruses, phosphorylation of viral proteins is invoked to regulate transcription, replication, and virus assembly (4–10).

Ebola virus (EBOV), a filovirus, causes severe hemorrhagic fever with high fatality rates and is mainly treated symptomatically due to the lack of approved antivirals. Nonetheless, promising EBOV inhibitors are currently at different stages of clinical development (11). In addition to antivirals that directly target viral enzymes or surface proteins, the development of inhibitors against proviral host cell factors has become an attractive option because it is suspected that such inhibitors are less prone to inducing resistance (12). However, to develop such host-targeting antivirals, it is necessary to understand the molecular mechanisms at the host-virus interface.

EBOV entry is accomplished by macropinocytosis, resulting in the release of viral nucleocapsids from the endosomal/lysosomal compartment into the cytoplasm (13). The nucleocapsid then acts as a template for primary transcription, which is executed by nucleocapsid-associated polymerase L, the polymerase cofactor VP35, and the transcription factor VP30 (14, 15). After viral mRNAs have been translated and sufficient amounts of viral proteins have been produced, replication and encapsidation of the genomic RNA occur. At the same time, secondary transcription takes place, which is distinct from primary transcription by the abundance of viral proteins. Although the precise mechanism by which VP30 supports primary and secondary transcription is unknown, it is clear that this function is regulated by the phosphorylation status of VP30 (10, 16). VP30 phosphorylation enhances its binding to the nucleoprotein NP while inhibiting its interaction with RNA and VP35, collectively resulting in the downregulation of viral transcription (10, 16–18). Interestingly, a nonphosphorylatable mutant of VP30 is sufficient to support secondary transcription, whereas primary transcription requires sequential phosphorylation and dephosphorylation (19). Six N-proximal serine residues of VP30 are potential phosphoacceptor sites. Intriguingly, a mutant of VP30 ($VP30^{29S}$) in which five of the six serine residues are replaced by alanine, with only serine 29 remaining, was found to be capable of supporting both primary and secondary transcription. Indeed, recombinant EBOV (recEBOV_29S) expressing $VP30^{29S}$ instead of wild-type VP30 ($VP30^{wt}$) was rescuable and behaved in a manner similar to that of wild-type EBOV (19), suggesting that reversible phosphorylation of serine 29 was necessary and sufficient to support all functions of VP30 during transcription.

Previous work has shown that the cellular phosphatases PP1 and PP2A are able to dephosphorylate VP30 (10, 18, 20). Dephosphorylation of VP30 by PP2A was found to be mediated by NP, which simultaneously recruited VP30 and PP2A into viral inclusion bodies via two adjacent binding motifs. The close proximity of VP30 and PP2A in association with NP results in efficient VP30 dephosphorylation and the consequent activation of EBOV transcription (21, 22).

Although VP30's site-specific dephosphorylation has been well elucidated, the nature of the VP30-specific kinase(s) and how and where VP30 phosphorylation occurs remain completely unknown. Using a proteomics approach, we identified two host kinases, serine-arginine protein kinase 1 (SRPK1) and SRPK2, that specifically phosphorylate the important residue serine 29 of VP30. Ectopic expression of SRPK1 enhanced VP30 phosphorylation and thus downregulated EBOV transcription, therefore reducing the propagation of infectious EBOV. Inhibition of endogenous SRPK1 downregulated primary transcription. We further identified the $R_{26}xxS_{29}$ motif in VP30 as a main SRPK1 recognition motif and confirmed the importance of this motif for viral growth. Together with the previously detected VP30-specific cellular phosphatase PP2A, the newly described VP30-specific kinase SRPK1 represents a phosphorylation/dephosphorylation circuit that regulates EBOV mRNA synthesis in viral inclusion bodies.

RESULTS

Identification of a VP30-specific cellular kinase. VP30 is phosphorylated at six N-proximal serine residues (Fig. 1A) (10); the most important is serine 29, the phosphorylation and dephosphorylation of which are necessary to ensure VP30's role in primary and secondary transcription (19).

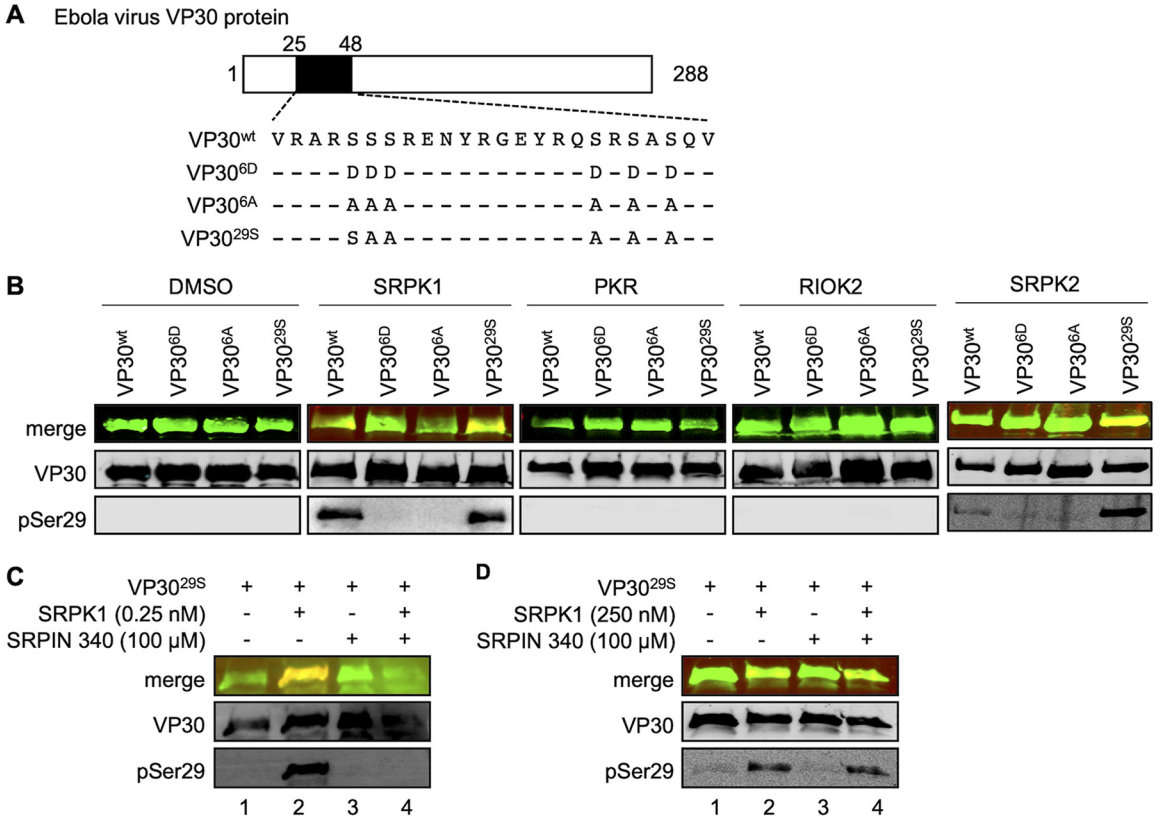

FIG 1 Identification of VP30-specific kinases. (A) Schematic drawing of Ebola virus VP30 showing amino acids 25 to 48 of VP30 and the mutants of VP30 employed. (B and C) Bacterially expressed MBP fusion proteins of VP30 (amino acids 8 to 272) or phosphomimetic mutants of VP30 were phosphorylated *in vitro* using recombinant SRPK1, PKR, RIOK2, and SRPK2. Samples were subjected to SDS-PAGE and Western blotting. VP30 and phosphorylated VP30 (serine 29) were detected using a guinea pig anti-VP30 and a rabbit anti-pSer29 antibody. (B) Bacterially expressed VP30 and mutants of VP30 were incubated with either DMSO (control), recombinant SRPK1, recombinant PKR, recombinant RIOK2, or recombinant SRPK2 in kinase reaction buffer for 30 min at room temperature. (C) Bacterially expressed $VP30^{29S}$ was incubated with either SRPK1 (0.25 nM), SRPIN340 (100 μM), or a mixture of SRPK1 (0.25 nM) and SRPIN340 (100 μM) in kinase reaction buffer for 18 h at room temperature. (D) Experimental setting as described above for panel C, except that the amount of recombinant SRPK1 was increased to 250 nM.

To identify the EBOV VP30-associated kinase(s), we adopted a proteomics approach by employing different versions of VP30: wild-type VP30 ($VP30^{wt}$), a nonphosphorylatable mutant of VP30 in which all six major phosphorylation sites at the N terminus are mutated to alanine ($VP30^{6A}$), a mutant that mimics fully phosphorylated VP30 via the replacement of the six serines to negatively charged aspartic acid residues ($VP30^{6D}$), and $VP30^{29S}$ (Fig. 1A) (10, 19). Ectopically expressed FLAG-tagged VP30 mutants were immunoprecipitated, and coprecipitating cellular proteins were eluted (16) and digested with trypsin prior to analysis by liquid chromatography-tandem mass spectrometry (MS/MS) (see Fig. S1 in the supplemental material) (23). A number of kinases coprecipitated with VP30 (Fig. 1B and Table S1); of these, we focused on SRPK1, interferon-induced double-stranded RNA-activated protein kinase (PKR), and serine/threonine protein kinase RIO2 (RIOK2). The three kinases displayed high binding with $VP30^{wt}$ and $VP30^{29S}$, with lower binding to $VP30^{6A}$ or the FLAG epitope alone (Fig. 1B and Table S1) (the original mass spectrometry data were deposited in the jPOST repository [accession numbers PXD016409 for ProteomeXchange and JPST000700 for jPOST]) (24). We then performed *in vitro* phosphorylation assays to examine whether the kinases are able to phosphorylate VP30. Bacterially expressed and purified VP30 mutants were incubated with the respective recombinant kinases in the presence of ATP, and VP30 phosphorylation was monitored using an anti-pSer29 antibody that specifically recognizes phosphorylated serine at position 29 (20). SRPK1 and the highly related SRPK2 clearly phosphorylated $VP30^{wt}$ and $VP30^{29S}$, whereas PKR and RIOK2 did

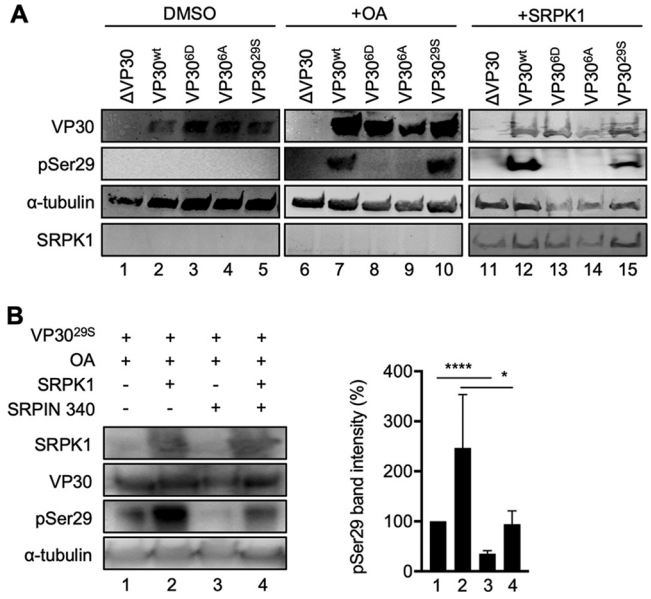

FIG 2 SRPK1 phosphorylation of VP30 in cells. (A) HEK293 cells expressing VP30 or mutants of VP30 were either treated with OA or transfected with a plasmid encoding SRPK1 and lysed at 24 h p.t. Cell lysates were subjected to SDS-PAGE and Western blotting using antibodies against VP30, pSer29, α-tubulin, and SRPK1. Lanes 1 to 5, DMSO-treated cells (control [ctrl]) incubated for 18 h; lanes 6 to 10, cells incubated with 25 nM OA (inhibitor of PP1/PP2A) for 18 h; lanes 11 to 15, VP30-expressing cells transfected with 500 ng of a plasmid encoding SRPK1. (B) Phosphorylation of VP30^{29S}. HEK293 cells expressing VP30^{29S} were treated with 25 nM OA and DMSO (control) (lane 1), 500 ng SRPK1 (lane 2), 30 μM SRPIN340 (lane 3), or both 500 ng SRPK1 and 30 μM SRPIN340 (lane 4). Quantification of the pSer29 band intensity in lanes 1 to 4 is shown in the graph. The pSer29 signal was normalized to the VP30 signal. The band intensity of the control (lane 1) was set to 100%. Numbers represent the means and SD of data from three independent experiments. Statistical analysis by a *t* test between lane 1 and either of the other lanes was applied. Asterisks indicate statistical significance (*, $P < 0.05$; ****, $P < 0.0001$).

not (Fig. 1B). To confirm that the phosphorylation of VP30 was specifically executed by SRPK1, we applied the SRPK1/SRPK2-specific inhibitor SRPIN340 (25), which resulted in a significant decrease in phospho-VP30^{29S} (Fig. 1C, lanes 3 and 4). Moreover, the inhibitory effect of SRPIN340 was dependent on its ratio to SRPK1, as increasing the amount of SRPK1 outcompeted the influence of SRPIN340 (Fig. 1D, lane 4). Altogether, mass spectrometry analyses, *in vitro* phosphorylation assays, and a specific inhibitor identified SRPK1 and SRPK2 as VP30-specific kinases able to phosphorylate the important serine at position 29 in VP30.

We then analyzed the intracellular phosphorylation of VP30 and found that VP30 was maintained in a nonphosphorylated state in the absence of phosphatase inhibitors (Fig. 2A, lanes 1 to 5). Indeed, phosphorylated VP30^{wt} and VP30^{29S} were observed only after treatment of VP30-expressing cells with okadaic acid (OA), an inhibitor of the VP30-specific phosphatases PP1 and PP2A (Fig. 2A, lanes 7 and 10). Similarly, phosphorylation of VP30^{wt} and VP30^{29S} was detected upon the ectopic expression of SRPK1, suggesting that the phosphatase activity acting on VP30 was outcompeted by SRPK1 overexpression and that the phosphorylation state of VP30 was shifted toward the phosphorylated form (Fig. 2A, lanes 12 and 15). Furthermore, the phosphorylation of VP30 was strongly increased when PP2A was inhibited by OA and SRPK1 was ectopically expressed (Fig. 2B, lanes 1 and 2), and VP30 phosphorylation was inhibited in the presence of OA and SRPIN340, indicating that SRPK1 is a major kinase that phosphorylates VP30 at serine 29 (Fig. 2B, lanes 2 and 3). As SRPIN340 treatment partially inhibited VP30 phosphorylation in the presence of ectopically expressed SRPK1, it appears that although the chosen concentration of SRPIN340 was sufficient to efficiently counteract endogenous SRPK1, it was not able to completely inhibit ectopically expressed SRPK1 (Fig. 2B, lanes 2 and 4). Quantification of the data from three independent experiments confirmed the statistical significance of the observations

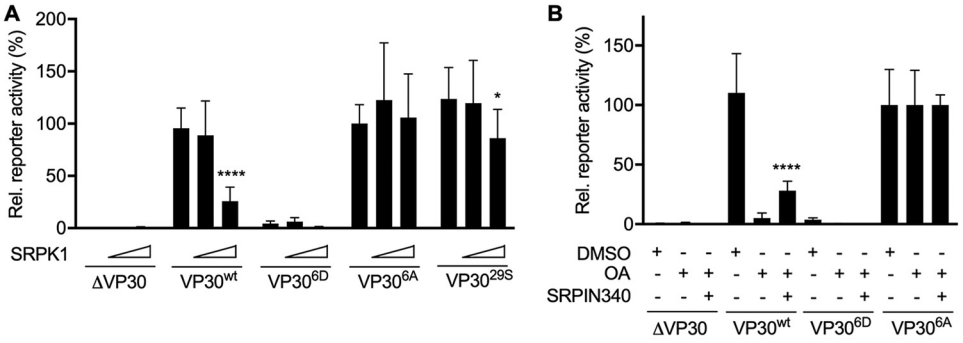

FIG 3 SRPK1 regulation of EBOV transcription/replication. (A) Dose-dependent effect of SRPK1 in the EBOV minigenome assay. HEK293 cells were transfected with plasmids encoding EBOV minigenome assay components (NP, VP35, L, the EBOV-specific minigenome, T7 polymerase, the absence or presence of each VP30 phenotype, and a plasmid encoding firefly luciferase for normalization). Different amounts of the SRPK1-encoding plasmid (0, 100, or 500 ng) were cotransfected. The results obtained with phosphorylation-independent $VP30^{6A}$ were set to 100%. Samples prepared in the absence of VP30 (ΔVP30) represent the baseline levels of the assay. Statistical analysis by a *t* test was applied between 0 ng of SRPK1-coding plasmid-transfected cells and either of the other treatments. (B) Effects of specific inhibition of SRPK1 by the inhibitor SRPIN340 on EBOV transcription/replication. HEK293 cells were transfected with plasmids encoding EBOV minigenome assay components (see above). At 30 h p.t., cells were incubated with either DMSO (control), 25 nM OA, or a mixture of 25 nM OA and 30 μM SRPIN340. At 48 h p.t., cells were lysed, and reporter gene activity was analyzed as indicated above for panel A. The means and SD from three independent experiments are indicated. Statistical analysis by a *t* test was applied between 25 nM OA and a mixture of 25 nM OA and 30 μM SRPIN340. Asterisks indicate statistical significance (*, $P < 0.05$; ****, $P < 0.0001$).

(Fig. 2B, graph). In summary, SRPK1 specifically phosphorylates $VP30^{wt}$ and $VP30^{29S}$ *in vitro* and in cultured cells and regulates the phosphorylation state of VP30 together with OA-sensitive phosphatases, likely PP2A and/or PP1.

SRPK1 regulates EBOV genome transcription/replication. We next used an EBOV-specific minigenome assay to analyze whether SRPK1 influences the transcriptional support activity of VP30 (14). The activity of SRPK1 was expected to promote the presence of phosphorylated VP30, which does not support transcription (10). Indeed, although the ectopic expression of SRPK1 had no effect on reporter gene levels in the presence of a nonphosphorylatable VP30 ($VP30^{6A}$), SRPK1 decreased reporter activities in the presence of $VP30^{wt}$ or $VP30^{29S}$ in a dose-dependent manner (Fig. 3A). As a negative control, we used the phosphomimetic mutant $VP30^{6D}$, which is unable to support viral transcription (10).

To monitor the effect of endogenous SRPK1, we used OA to inhibit the highly active VP30-specific phosphatases PP2A and PP1, which resulted in hyperphosphorylated VP30 (Fig. 2A) and consequently decreased $VP30^{wt}$-mediated reporter gene activity by more than 90% (Fig. 3B) (10, 19). Treatment of cells with both OA and SRPIN340 partially restored reporter gene activity (Fig. 3B), indicating that SRPK1 and PP2A and/or PP1 together target VP30, determine VP30's phosphorylation status (as shown in Fig. 2B), and, consequently, regulate viral transcription (19, 20). In the absence of OA and, thus, in the presence of VP30-specific phosphatase activity, inhibition of endogenous SRPK1 by SRPIN340 had no effect on secondary viral transcription/replication (Fig. S2). This result was consistent with previous reports demonstrating that VP30 is efficiently dephosphorylated by PP2A in the presence of NP, resulting in a highly active VP30 and efficient secondary viral transcription in a minigenome assay (20, 22). Therefore, it was not surprising that the already dephosphorylated VP30 could not be further activated by the inhibition of endogenous SRPK1. To evaluate the cytotoxicity of SRPIN340, we performed cell viability assays in the presence of increasing concentrations of the inhibitor (Fig. S3). Cytotoxicity was negligible at the selected concentration (30 μM), as previously reported (25, 26).

Together, these findings indicate that SRPK1 plays an important role in EBOV transcription/replication by modulating the VP30 phosphorylation status.

Role of VP30 phosphorylation in primary transcription. To investigate the functional significance of VP30 phosphorylation by endogenous SRPK1/SRPK2 for

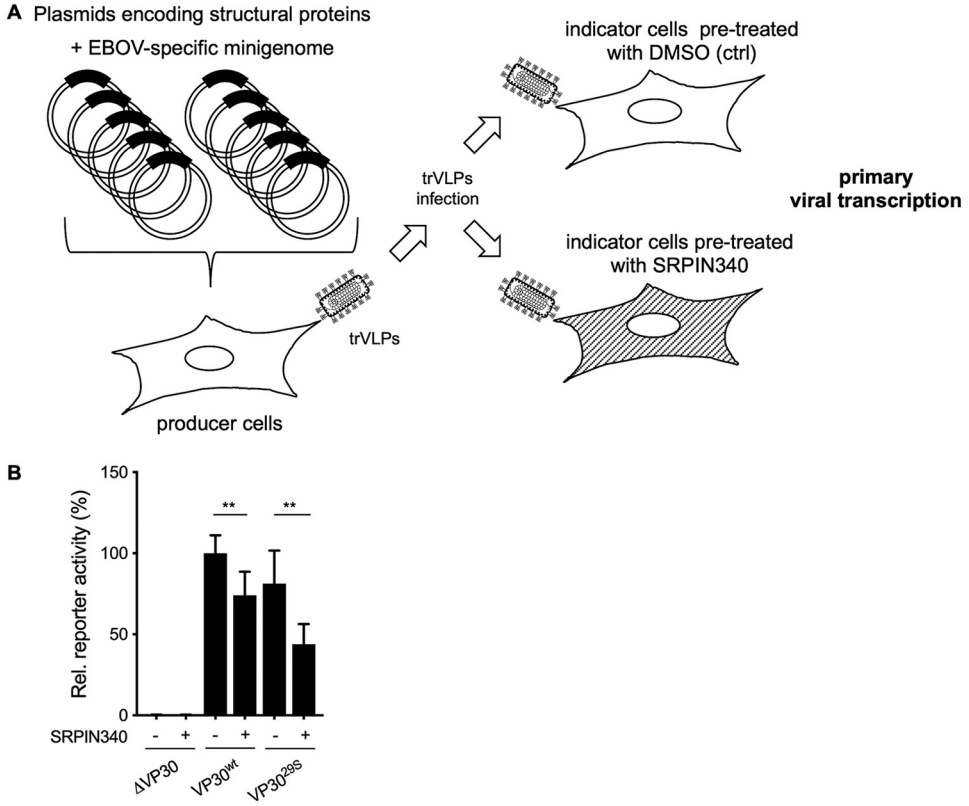

FIG 4 Role of SRPK1-mediated VP30 phosphorylation in primary transcription. (A) Schematic of the EBOV transcription- and replication-competent virus-like particle (trVLP) assay. HEK293 cells (producer cells) were transfected with plasmids expressing all of the viral structural proteins and an EBOV-specific minigenome encoding *Renilla* luciferase together with a plasmid encoding firefly luciferase for normalization. The replicated minigenomes are released in the form of virus-like particles (trVLPs) into the supernatant, which was collected and purified via a sucrose cushion at 72 h p.t. Huh-7 cells, the indicator cells, were pretreated with either DMSO (control) or 30 μM SRPIN340 for 24 h. The purified trVLPs were used to infect pretreated Huh-7 cells, and reporter gene activities were measured at 48 h p.t. (B) Relative reporter activities in indicator cells at 48 h p.i. The luciferase activity of VP30^{wt}-expressing cells treated with DMSO was set to 100%. Samples prepared in the absence of VP30 (ΔVP30) represent the baseline levels of the assay. The means and SD from three independent experiments are indicated. Statistical analysis by a *t* test was applied between control- and SRPIN340-treated cells. Asterisks indicate statistical significance (*, $P < 0.05$; ***, $P < 0.001$).

primary transcription, we used an EBOV-specific transcription- and replication-competent virus-like particle (trVLP) assay. All EBOV proteins and an EBOV-specific minigenome were ectopically expressed, resulting in the formation of nucleocapsid-like structures that were transported to the plasma membrane and released into the supernatant in the form of trVLPs. The released trVLPs were used to infect fresh target cells (indicator cells) to monitor primary viral transcription (Fig. 4A) (27–29). Here, we compared SRPIN340-treated with mock-treated indicator cells. Interestingly, treatment with SRPIN340 decreased the reporter gene activities for trVLPs that contained VP30^{wt} to 78% and for trVLPs that contained VP30^{29S} to 53% (Fig. 4B). Although the inhibitory activity of SRPIN340 was statistically significant, primary transcription was not completely blocked, suggesting the existence of additional VP30-specific kinases. This result is consistent with an important role of SRPK1 or SRPK2 for the efficient primary transcription of EBOV (19).

SRPK1 activity regulates EBOV infection. Subsequently, we analyzed the effect of ectopically expressed SRPK1 on EBOV infection using recombinant EBOVs expressing either VP30^{wt} (recEBOV_wt) or VP30^{29S} (recEBOV_29S) (19). Plasmids encoding SRPK1 were transfected into HEK293 or Huh-7 cells 12 h prior to EBOV infection, and cell supernatants were collected at 1 and 2 days postinfection (p.i.). The titer of infectious EBOV in the supernatants was determined using a 50% tissue culture infectious dose

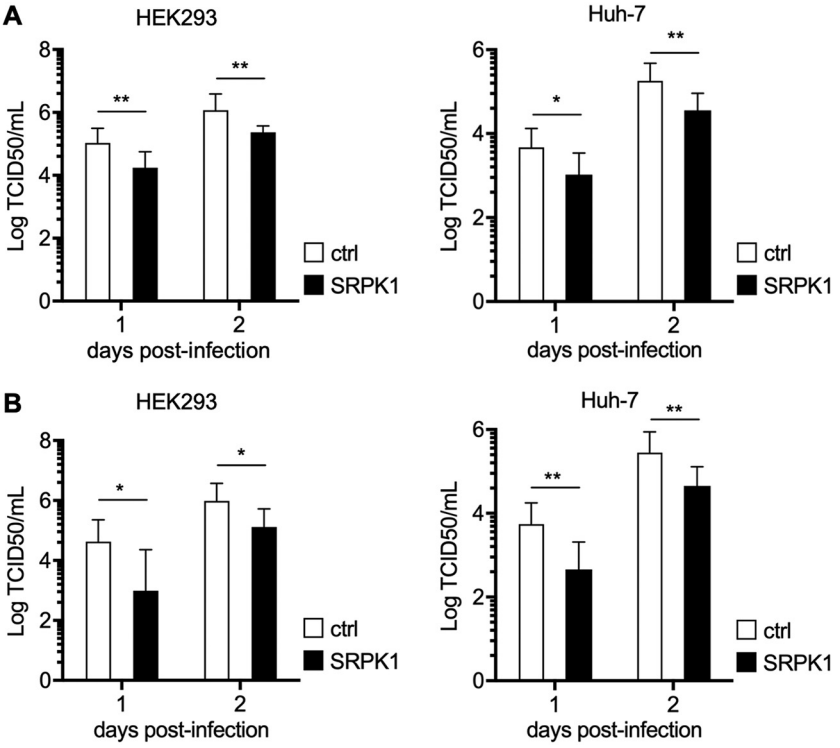

FIG 5 Influence of ectopic expression of SRPK1 on EBOV infection. HEK293 or Huh-7 cells were transfected with the SRPK1-encoding plasmid 12 h prior to infection with recEBOV_wt or recEBOV_29S at an MOI of 0.1. Cell supernatants were collected at 1 and 2 days p.i. for titration of the number of infectious virus particles released ($TCID_{50}$). The means and SD of data from three independent experiments carried out with recEBOV_wt (A) and recEBOV_29S (B) are displayed. Statistical analysis by a *t* test was applied between control- and SRPIN340-treated cells. Asterisks indicate statistical significance (*, $P < 0.05$; **, $P < 0.01$).

($TCID_{50}$) assay (30). The ectopic expression of SRPK1 in HEK293 cells and Huh-7 cells resulted in a reduction in the virus titer by approximately 1 log (Fig. 5A and B), suggesting that a shift in the phosphorylation state of VP30 toward hyperphosphorylation impaired EBOV propagation.

Characterization of the interaction between VP30 and SRPK1. The recognition motif for SRPK1 has not been clearly identified. However, the motif RxxS, which is present three times in the N-proximal serine clusters of VP30, is a consensus sequence for many kinases (31, 32) (Fig. 6A). Previous work revealed that serines 29 and 31 of VP30 are the main phosphoacceptor sites that influence its transcriptional activity (19). Both serines are located in an RxxS motif. Conversely, serine 42, which is also part of an RxxS motif, does not appear to be involved in regulating transcription (19).

To investigate whether SRPK1 recognizes serine residues of VP30 within an RxxS motif, we focused on the $R_{26}ARS_{29}$ motif, including the key serine at position 29 (19, 20). A mutant of $VP30^{29S}$ was constructed by replacing arginine 26 with alanine ($VP30^{26A29S}$) (Fig. 6A), with the expectation that $VP30^{26A29S}$ would not be phosphorylated by kinases that recognize the RxxS motif as a substrate. *In vitro* phosphorylation assays showed that recombinant SRPK1 efficiently phosphorylated $VP30^{29S}$ but not $VP30^{26A29S}$ (Fig. 6B, lane 3 versus lane 4). When $VP30^{29S}$ or $VP30^{26A29S}$ was ectopically expressed in HEK293 cells, neither protein was phosphorylated, indicating that endogenous SRPK1 was not sufficient to counteract the activity of PP2A, supporting the results presented in Fig. 2A (Fig. 6C, lanes 1 and 2). However, when the phosphatases were inhibited by OA, $VP30^{29S}$ was phosphorylated, but $VP30^{26A29S}$ was not (Fig. 6C, lane 3 versus lane 4). Moreover, the ectopic coexpression of SRPK1 resulted in phosphorylated $VP30^{29S}$ but not phosphorylated $VP30^{26A29S}$ (Fig. 6C, lane 5 versus lane 6). These results suggest that

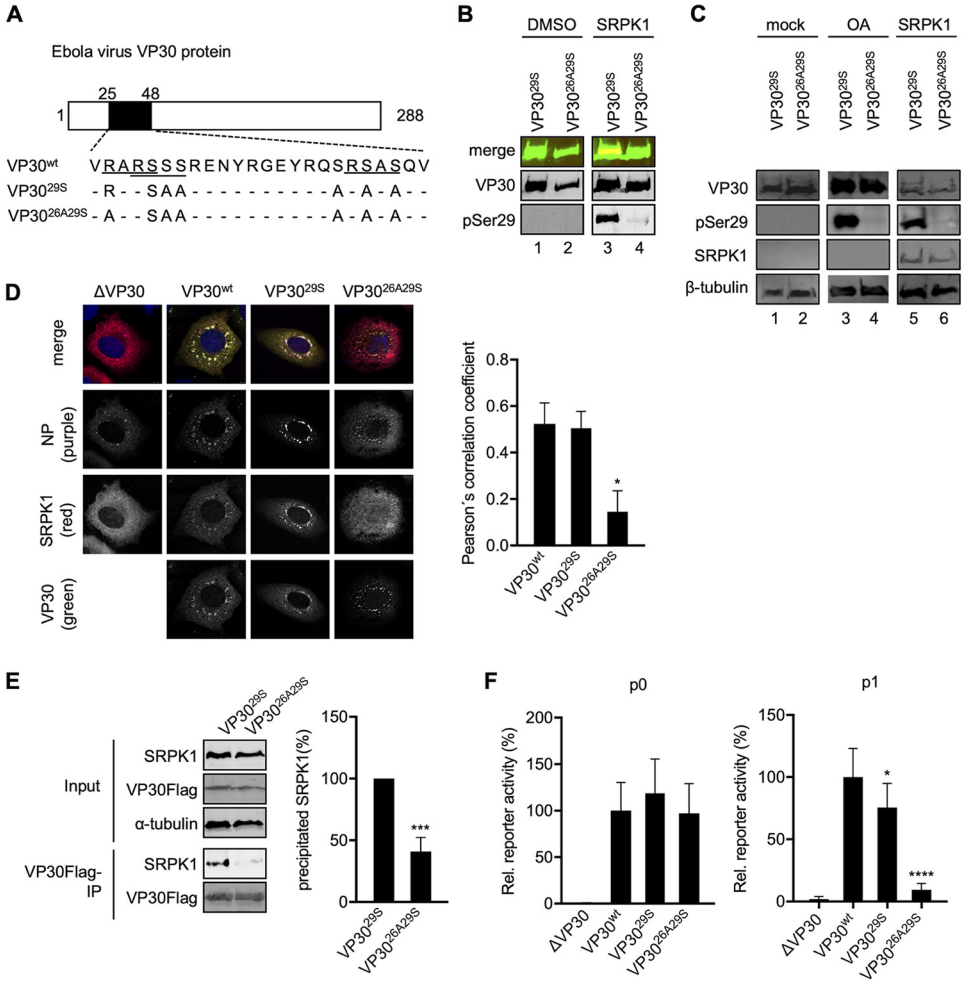

FIG 6 Impact of the SRPK1-binding motif $R_{26}xxS_{29}$ on the activity of VP30 in EBOV transcription and growth. (A) Schematic drawing of Ebola virus VP30 showing amino acids 25 to 48 of VP30 and mutants of VP30. (B) *In vitro* phosphorylation of purified $VP30^{29S}$ or $VP30^{26A29S}$ by SRPK1 (Fig. 1B). (C) SRPK1 coexpression affects the phosphorylation status of S29. HEK293 cells were transfected with plasmids encoding $VP30^{wt}$, $VP30^{29S}$, or $VP30^{26A29S}$. Cells were either treated with DMSO (control) or OA or transfected with 500 ng of a plasmid encoding SRPK1. Cell lysates were subjected to SDS-PAGE and Western blotting. (D) Huh-7 cells transfected with plasmids encoding NP, SRPK1, SRPK1-TagRFP, and either $VP30^{wt}$, $VP30^{29S}$, or $VP30^{26A29S}$ were fixed at 24 h p.t. and analyzed by confocal immunofluorescence microscopy. The intracellular distributions of NP, SRPK1, and VP30 were analyzed using specific antibodies and autofluorescence (SRPK1-TagRFP). The graph shows the quantification of colocalization signals by Pearson's correlation coefficients for SRPK1 and VP30. The means and standard errors (SE) from 16 images derived from three independent experiments are shown. One-way ANOVA was applied among $VP30^{wt}$, $VP30^{29S}$, and $VP30^{26A29S}$, and a statistical difference was found between $VP30^{26A29S}$ and the others. (E) HEK293 cells were transfected with plasmids encoding SRPK1 and FLAG-tagged $VP30^{29S}$ or FLAG-tagged $VP30^{26A29S}$ proteins. At 48 h p.t., the cells were lysed, and protein complexes were precipitated using mouse anti-FLAG M2 agarose. An aliquot of the cell lysates (input) was collected before precipitation. Precipitates and input cell lysates were analyzed by SDS-PAGE and Western blotting using SRPK1-, FLAG-, and α-tubulin-specific antibodies. In the graph, the amount of coprecipitated SRPK1 is indicated as a percentage. The amount of SRPK1 coprecipitated by $VP30^{29S}$ was set to 100%. The means and SD from 3 independent experiments are indicated. Statistical analysis by a *t* test was applied between $VP30^{29S}$ and $VP30^{26A29S}$. (F) HEK293 cells were transfected with plasmids encoding trVLP assay components. Relative reporter activities are shown in p0 producer cells (analyzed at 72 h p.t.) and p1 indicator cells (analyzed at 48 h p.i.). The luciferase activity of $VP30^{wt}$-expressing cells was set to 100%. The means and SD from three independent experiments are indicated. Statistical analysis by a *t* test was applied between $VP30^{wt}$ and the others. Asterisks indicate statistical significance (*, $P < 0.05$; ***, $P < 0.001$; ****, $P < 0.0001$).

the replacement of the arginine at position 26 by alanine destroyed the substrate sequence of SRPK1 as well as any other potential VP30-specific kinases that phosphorylate serine 29. To substantiate these findings, we analyzed the intracellular distributions of VP30 and SRPK1 by immunofluorescence and their interaction by coimmunoprecipitation (co-IP) assays. In the presence of NP, VP30 was recruited into NP-induced

inclusion bodies; in contrast, the expression of VP30 alone resulted in a homogenous cytoplasmic distribution (10). Upon the coexpression of NP and SRPK1, the latter was diffusely distributed in the cytoplasm, whereas NP was detected mainly in perinuclear inclusions (Fig. 6D). However, when we additionally expressed $VP30^{wt}$ or $VP30^{29S}$, SRPK1 was recruited into inclusion bodies together with VP30. In contrast, when $VP30^{wt}$ was replaced by $VP30^{26A29S}$, SRPK1 was not recruited into the NP-induced inclusions (Fig. 6D). Quantification of VP30 and SRPK1 colocalization revealed a high Pearson's correlation coefficient for $VP30^{wt}$ and $VP30^{29S}$ (0.52 and 0.50, respectively), which was significantly reduced for $VP30^{26A29S}$ (0.14) (Fig. 6D, right). These results indicate that SRPK1 was corecruited by VP30 into NP-induced inclusion bodies depending on the intact $R_{26}xxS_{29}$ motif. To confirm the interaction between SRPK1 and VP30, we performed coimmunoprecipitation analyses of ectopically expressed SRPK1 and $VP30^{29S}$ or $VP30^{26A29S}$ and found that $VP30^{26A29S}$ precipitated significantly less SRPK1 than did $VP30^{29S}$ (Fig. 6E).

Next, we analyzed the impact of a mutated $R_{26}xxS_{29}$ motif with the trVLP assay (27). While the mutated kinase recognition motif in $VP30^{26A29S}$ had no impact on secondary transcription in producer cells (Fig. 6F), primary transcription in indicator cells was significantly reduced when the cells were infected with VLPs containing $VP30^{26A29S}$ (Fig. 6F).

These results emphasize the significance of serine 29 as a target of phosphorylation/dephosphorylation processes to regulate primary viral transcription and also identify arginine 26 as a crucial residue for serine 29 phosphorylation by kinases recognizing RxxS motifs, such as SRPK1.

Impact of the kinase recognition motif $R_{26}xxS_{29}$ of VP30 on EBOV propagation. To analyze the influence of the $R_{26}xxS_{29}$ motif during EBOV infection, we employed three different recombinant EBOVs, encoding either $VP30^{26A29S}$, $VP30^{29S}$, or $VP30^{wt}$ (recEBOV_26A29S, recEBOV_29S [19], and recEBOV_wt). Based on the results shown in Fig. 6, recEBOV_26A29S should not be able to functionally interact with SRPK1 or other kinases that recognize the RxxS motif. In fact, compared to recEBOV_wt (Fig. 7A, circles) and recEBOV_29S (squares), viral titers in the supernatants of infected HEK293 cells were reduced by up to 2 to 3 logs for recEBOV_26A29S (triangles) (multiplicity of infection [MOI] of 0.1). Strongly reduced growth for recEBOV_26A29S in comparison to recEBOV_wt and recEBOV_29S was also detected in Huh-7 cells (Fig. 7B). These results were confirmed using a lower MOI (0.01) (Fig. S4). In addition, electron microscopic analyses showed that all three recombinant viruses were morphologically indistinguishable (Fig. 7C). Furthermore, colocalization analysis of VP30 and SRPK1 in cells infected with the recombinant EBOVs revealed high Pearson's correlation coefficients for recEBOV_wt- and recEBOV_29S-infected cells (0.48 and 0.55, respectively), but the correlation coefficient was reduced for recEBOV_26A29S-infected cells (0.18) (Fig. 7D). These findings indicate an impaired interaction between VP30 and SRPK1 in recEBOV_26A29S infection. As we have shown that $VP30^{26A29S}$ is active in a minigenome assay where only secondary transcription of a single gene is monitored, the observed inhibition of recEBOV_26A29S is most likely due to the interruption of primary transcription in newly infected cells, possibly by inhibiting the reinitiation of mRNA synthesis at internal genes.

Overall, these results indicate that SRPK1 interacted directly with VP30 and was recruited into NP-induced inclusion bodies in EBOV-infected cells. SRPK1 specifically recognized and phosphorylated serine 29 of VP30 in a manner dependent on the $R_{26}xxS_{29}$ motif, which is conserved among all Ebola viruses. SRPK1 activity regulated EBOV transcription, and mutation of the substrate motif significantly inhibited the growth of recombinant EBOVs containing serine 29 as the only phosphorylatable site at the N terminus of VP30. Thus, SRPK1 is an important VP30-specific kinase contributing to the complex phosphorylation/dephosphorylation steps involved in EBOV transcription.

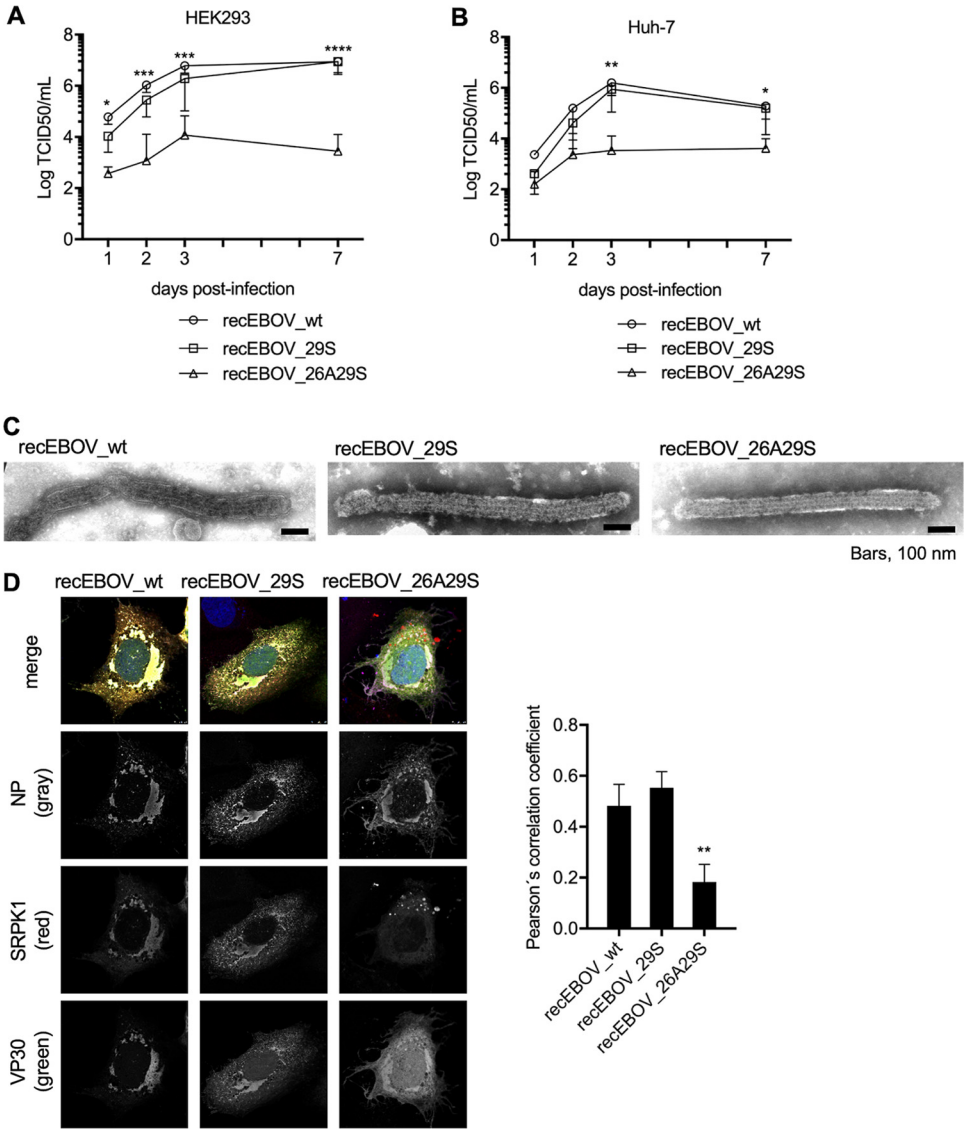

FIG 7 Defective replication of recEBOV_26A29S. (A and B) HEK293 (A) or Huh-7 (B) cells were infected (MOI of 0.1) with either recEBOV_wt, recEBOV_29S, or recEBOV_26A29S. The inoculum was removed at 1 h p.i., and cell supernatants were collected at 1, 2, 3, and 7 days p.i. for titration of infectious virus particles released ($TCID_{50}$). The means and SD from three independent experiments are indicated. One-way ANOVA was applied among recEBOV_wt, recEBOV_29S, and recEBOV_26A29S, and statistical differences were found between recEBOV_26A29S and the others. (C) Electron microscopy analyses of released viral particles. HEK293 cells were infected with either recEBOV_wt, recEBOV_29S, or recEBOV_26A29S. Cell supernatants were collected at 48 h p.i., and viral particles were purified via ultracentrifugation and fixed with paraformaldehyde. Samples were subjected to negative staining and analyzed by transmission electron microscopy. (D) Huh-7 cells expressing SRPK1 and SRPK1-TagRFP were infected with recEBOV_wt, recEBOV_29S, or recEBOV_26A29S. After 1 h of infection, the inoculum was removed, and the cells were fixed at 24 h p.i. for analysis of the intracellular distribution of NP, VP30, and SRPK1 by confocal immunofluorescence microscopy. The graph shows the quantification of colocalization signals by Pearson's correlation coefficients for SRPK1 and VP30. The means and SE from 16 images derived from 3 independent experiments are shown. A Kruskal-Wallis test was applied among recEBOV_wt, recEBOV_29S, and recEBOV_26A29S, and statistical differences were found between recEBOV_26A29S and the others. Asterisks indicate statistical significance (*, $P < 0.05$; **, $P < 0.01$; ***, $P < 0.001$; ****, $P < 0.0001$).

DISCUSSION

EBOV VP30 has been described as a viral phosphoprotein, and recent studies showed that phosphorylation of VP30 needs to be tightly regulated (10, 15, 16, 18). Nonphosphorylated VP30 is essential and sufficient to support secondary transcription in an EBOV-specific minigenome system, and indeed, the majority of VP30 molecules in EBOV-infected cells are nonphosphorylated (20). Importantly, however, phosphorylat-

able serine residues near the N terminus of VP30 are still necessary and sufficient to support primary viral transcription as well as the reinitiation of VP30-mediated transcription at internal EBOV genes (19, 33). Serine residue 29 is most important in this respect (19). Thus, a cycle of phosphorylation and dephosphorylation events is key to supporting the transcriptional activity of EBOV VP30 (10, 16, 19, 33).

The present study builds on these observations, demonstrating that SRPK1 and SRPK2 were able to phosphorylate VP30, and the SRPK1/2-specific inhibitor SRPIN340 significantly reduced the phosphorylation of serine 29 (Fig. 1 and 2). In addition, SRPIN340 inhibited primary viral transcription in an EBOV-specific trVLP assay, indicating the biological relevance of SRPK1-mediated phosphorylation of VP30 (Fig. 4B).

We show that SRPK1 uses the kinase recognition motif $R_{26}ARS_{29}$ to phosphorylate serine 29 of VP30 and as a tool for its recruitment into the EBOV inclusion bodies where transcription and replication take place. The $R_{26}xxS_{29}$ motif is conserved among all ebolavirus species (see Fig. S5 in the supplemental material), indicating an important role for the function of VP30. Indeed, our study demonstrated that mutation of the $R_{26}ARS_{29}$ motif in recombinant EBOV excluded SRPK1 from the inclusion bodies and dramatically impaired EBOV propagation (Fig. 7A, B, and D and Fig. S4).

SRPK1 and SRPK2 are cellular kinases that shuttle between the cytosol and nucleus and target proteins containing serine-arginine-rich domains (SR proteins) (for a review, see reference 34). It has been reported that SRPK1 also phosphorylates viral proteins (35–39). For example, SRPK1 is recruited by the E1^E4 proteins of human papillomaviruses and the ICP27 protein of herpes simplex virus 1, resulting in the downregulation of host SR protein phosphorylation (35, 37). With regard to RNA viruses, inhibition of SRPK1 by SRPIN340 suppresses hepatitis C virus and human immunodeficiency virus replication, although these effects might be caused by modulation of RNA splicing through alteration of the SR protein phosphorylation status (25, 26).

The results presented here complement previous studies on the role of the cellular phosphatase PP2A that specifically dephosphorylates NP-associated VP30 (22). We presume that there is a delicate interplay between PP2A and SRPK1/SRPK2 to regulate primary and secondary transcription of EBOV (22).

Figure 8 shows the current working model of how VP30 can be phosphorylated and dephosphorylated to ensure its function in EBOV transcription. Nucleocapsid-associated VP30 in released virions is phosphorylated (15). Once the virus envelope has fused with the endosomal/lysosomal membrane during the entry process and the nucleocapsid has entered the cytoplasm, phosphorylated VP30 is dephosphorylated by PP2A, which is recruited via its subunit B56 to the LxxIxE motif of NP in close proximity to the VP30-binding motif PPxPxY (21, 22) (Fig. 8, panel 1 [the boxed area illustrates the location of the binding motifs on NP]). Dephosphorylation weakens binding between VP30 and NP, and released dephosphorylated VP30 is directed toward the first transcriptional start site of the viral RNA (tss-NP) (Fig. 8, panel 2) (40–42). At tss-NP, VP30 recruits the polymerase complex via binding of VP35 (16, 43) and initiates transcription (Fig. 8, panel 3). Subsequently, VP30 is phosphorylated by SRPK1 and thereby is released from its interaction with RNA and VP35 (Fig. 8, panel 3, boxed area) (17). After another round of dephosphorylation by NP-associated PP2A (Fig. 8, panel 4), VP30 moves to the next transcription start site (tss-VP35) to reinitiate the transcription of the second gene (Fig. 8, panel 5). Overall, the interplay of SRPK1 and PP2A is presumed to provide a full regulatory circuit to ensure VP30's activity in primary EBOV transcription.

MATERIALS AND METHODS

Cell culture. Huh-7 (human hepatoma), HEK293 (human embryonic kidney), and Vero E6 (African green monkey kidney) cells were maintained in Dulbecco's modified Eagle medium (DMEM; Life Technologies) supplemented with 10% (vol/vol) fetal bovine serum (FBS; PAN Biotech), 5 mM L-glutamine (Q; Life Technologies), and 50 U/ml penicillin and 50 μg/ml streptomycin (PS; Life Technologies) and grown at 37°C with 5% CO_2.

Plasmids. All plasmids coding for wild-type EBOV proteins (pCAGGS-NP, -VP35, -VP40, -GP, -VP30, -VP24, and -L), the EBOV-specific minigenome (3E5E-luc), and pCAGGS-T7 polymerase have been described previously (14, 27). The plasmids pCAGGS-VP30^{29S}, -VP30^{6D}, and -VP30^{6A} were also described previously (10, 19). Cloning of pCAGGS-VP30^{26A29S} was performed with a multisite-directed mutagenesis

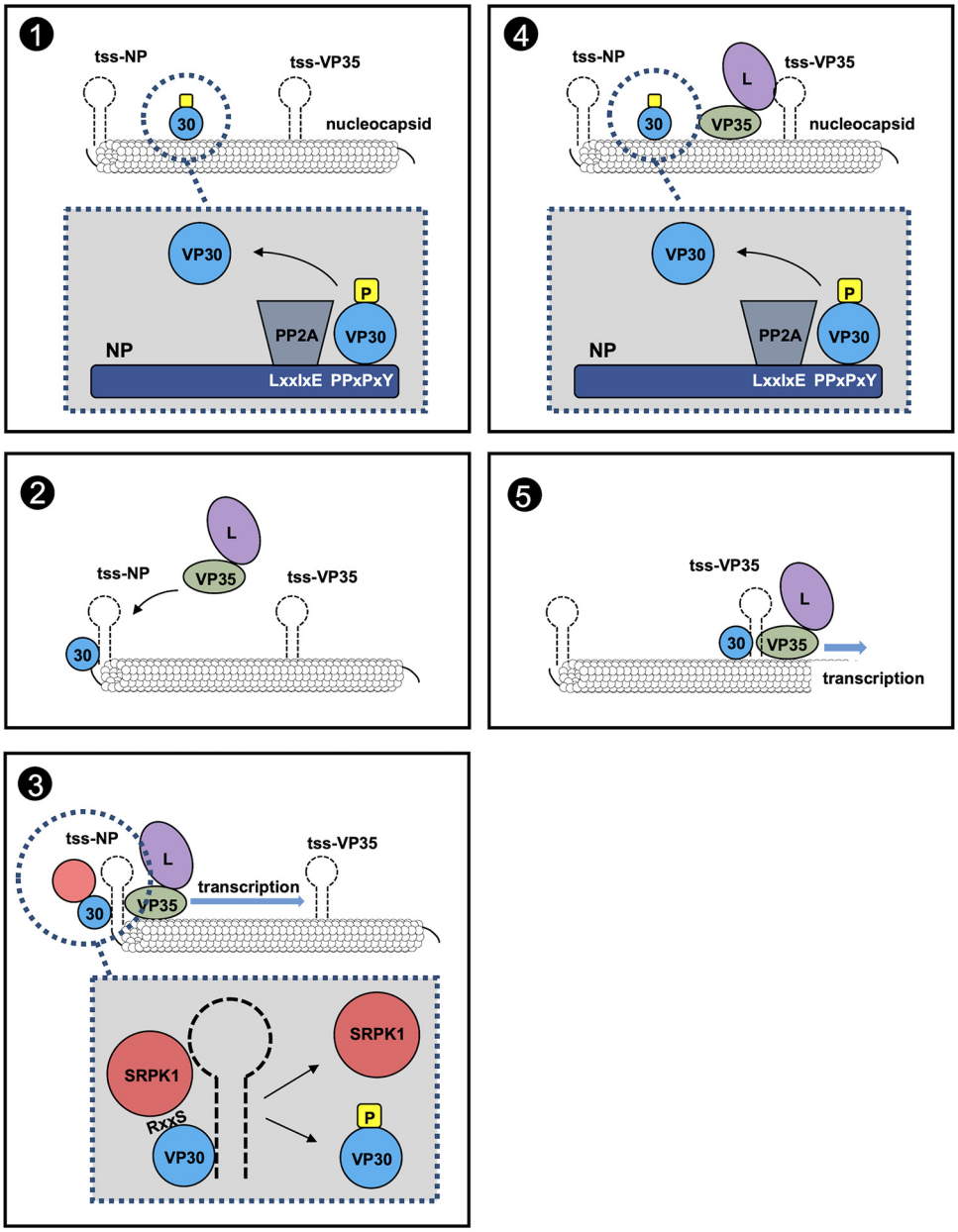

FIG 8 Model of VP30 reversible phosphorylation during the EBOV replication cycle. NP expression induces inclusion body formation. A sequence of phosphorylation and dephosphorylation events is essential for a fully functional VP30 in primary and secondary transcription. Within NP-induced inclusion bodies, SRPK1 is corecruited with VP30, which harbors SRPK1 recognition sites at its N-terminal site (1). EBOV NP recruits subunit B56 of the cellular phosphatase PP2A by interaction with a motif in the direct vicinity of the VP30-binding site. VP30 is dephosphorylated (2), associates with the polymerase cofactor VP35 by RNA interaction, and clamps the RNA template together with polymerase L and VP35 (3). Transcription of viral RNA is initiated. The host kinase SRPK1, recruited to the viral inclusions by VP30 through interaction of the conserved RxxS motif in Ebola viruses, enables the transient phosphorylation of VP30. Phosphorylated VP30 loses its RNA-binding affinity, dissociates from the polymerase complex (4), and binds to NP before again being dephosphorylated by PP2A and redirected to the second transcriptional start site to reinitiate the transcription of the second gene (5). The interplay of SRPK1 and PP2A provides a full regulatory circuit to ensure VP30's activity in EBOV transcription. Letters in the NP helix emphasize the PP2A-B56-binding motif LxxIxE and the VP30-binding motif PPxPxY. tss, transcription start site.

kit (Agilent) according to the manufacturer's recommendations. Construction of the pBADM41/VP30$_{8-272}$ variant plasmids (VP30^{wt}, VP30^{6D}, VP30^{6A}, VP30^{29S}, and VP30^{26A29S}) used for bacterial purification of maltose-binding protein (MBP)-VP30$_{8-272}$ was described previously (17). Human SRPK1 DNA was derived from pDONR223-SRPK1, a gift from William Hahn and David Root (Addgene plasmid 23582), and cloned into pCAGGS vector plasmids. TagRFP-SRPK1 derivatives were produced by using a ligation PCR

technique as indicated previously (44). All constructs were verified by sequencing. Primer sequences are available upon request.

Coimmunoprecipitation and mass spectrometric analysis. Co-IP of EBOV components was carried out as previously described (16), with the following modifications. For coimmunoprecipitation, HEK293 cells in 6-well plates were transfected with 500 ng/well of each protein-coding plasmid by using TransIT (Mirus). After 48 h, cells were lysed with 500 μl of ice-cold coimmunoprecipitation lysis buffer (20 mM Tris-HCl, 100 mM NaCl, 1% Nonidet P-40, 17.5 mM EDTA, and 0.1% Triton X-100 [pH 7.5] with Complete protease inhibitor mixture [Roche]) for 20 min at room temperature and then subjected to sonication three times for 20 s each at 4°C (Branson 450 sonifier). The clarified supernatant was added to 45 μl of equilibrated mouse anti-FLAG M2 affinity gel agarose (Sigma-Aldrich). The reaction mixture was incubated overnight at 4°C on a laboratory rotator. Elution of precipitates was achieved with 60 μl of elution buffer (125 mM Tris-HCl, 2% SDS [pH 6.8]) for 5 min at room temperature and subjected to 95°C for 3 min. The agarose beads were completely removed by two rounds of centrifugation (14,000 rpm for 5 min at 4°C). The final supernatant was subjected to SDS-PAGE.

Samples for mass spectrometry were prepared as follows. HEK293 cells (150-cm^2 dish) were transfected with 6 μg of each protein-coding plasmid by using TransIT (Mirus). Cell lysis and elution were performed as described above. For loading the samples onto an SDS-PAGE gel, glycerol was added to the eluted supernatants, and PAGE was started. Immediately after samples had entered the separation gel, electrophoresis was stopped. After staining the gel with colloidal Coomassie, the protein bands were excised and subjected to in-gel digestion with trypsin (45). Mass spectrometric analysis was performed as described previously (46), using an Orbitrap Velos Pro mass spectrometer (Thermo Fisher Scientific), which was connected online with a nano-C_{18} column-equipped Ultimate nano-RSLC-HPLC (rapid-separation liquid chromatography-high performance liquid chromatography) system (Dionex). An aliquot of 15 μl of the tryptic digest was injected onto a C_{18} preconcentration column, and automated trapping and desalting of the sample were performed at a flow rate of 6 μl/min using water–0.05% formic acid as the solvent.

Tryptic peptides were separated with water–0.045% formic acid and 80% acetonitrile–0.05% formic acid at a flow rate of 300 nl/min. The column was connected to a stainless steel nanoemitter (Proxeon, Denmark), and the eluent was sprayed directly toward the heated capillary of the mass spectrometer using a potential of 2,300 V. A survey scan with a resolution of 60,000 within the Orbitrap mass analyzer was combined with at least three data-dependent MS/MS scans with dynamic exclusion for 30 s using either CID (collision-induced dissociation) with the linear ion trap or HCD (higher-energy collisional dissociation) and orbitrap detection at a resolution of 7,500. Data analysis was performed using Proteome Discoverer (v4.0; Thermo Fisher Scientific) with the SEQUEST and MASCOT (v2.4; Matrix Science) search engines using either the Swiss-Prot or NCBI database (47).

Expression and purification of maltose-binding protein fusion proteins. The procedures for the expression and purification of MBP-VP30$_{8-272}$ proteins (MBP-VP30^{wt}, -VP30^{6D}, -VP30^{6A}, -VP30^{29S}, and -VP30^{26A29S}) were described previously (17). The purity of the protein was analyzed by SDS-PAGE and Coomassie blue staining. The protein concentration was measured by using a Pierce Coomassie (Bradford) protein assay kit (Thermo Fisher Scientific).

Phosphorylation detection assay *in vitro* and in cells. The *in vitro* reaction between each purified mutant of VP30 (VP30^{wt}, VP30^{6D}, VP30^{6A}, VP30^{29S}, and VP30^{26A29S}) and the employed kinases was analyzed using 20 μl of kinase reaction buffer (40 mM Tris-HCl, 20 mM $MgCl_2$, 0.1 mg/ml bovine serum albumin [BSA] [pH 7.5]) with 2 mM ATP. Recombinant SRPK1 and PKR were purchased from Thermo Fisher Scientific, and RIOK2 was purchased from Abcam. Okadaic acid (OA; Calbiochem) and SRPIN340 (Sigma-Aldrich) were dissolved in dimethyl sulfoxide (DMSO) according to the manufacturers' recommendations. A phosphospecific antibody recognizing specifically VP30 phosphorylated at serine 29 (anti-pS29) was used for the evaluation of VP30 phosphorylation (20).

The impact of endogenous kinases on the phosphorylation of VP30 was analyzed in HEK293 cells (6-well plate, seeded with 8×10^5 cells/well) transfected with 500 ng of each plasmid encoding VP30 and mutants of VP30 (pCAGGS-VP30^{wt}, -VP30^{6D}, -VP30^{6A}, -VP30^{29S}, and -VP30^{26A29S}). At 48 h posttransfection (p.t.), cells were lysed in TMT buffer (50 mM Tris-HCl, 5 mM $MgSO_4$, 1 mM dithiothreitol [DTT], 0.5% Triton X-100 [pH 7.5]) with or without a phosphatase inhibitor (25 nM OA [Sigma-Aldrich] with 2 mM ATP [Sigma-Aldrich]) and incubated for 1 h at 37°C. The reaction mixture was sonicated three times for 20 s each and subsequently spun down at 14,000 rpm at 4°C for 10 min. The supernatants were subjected to Western blot analyses. The effect of ectopically expressed SRPK1 on the phosphorylation of VP30 was analyzed in HEK293 cells expressing the different VP30 mutants (see above), which were cotransfected with 500 ng of pCAGGS-SRPK1. At 48 h p.t., cells were lysed in TMT buffer for 20 min at room temperature and subsequently sonicated three times for 20 s each. After centrifugation at 14,000 $\times$ *g* at 4°C for 10 min, supernatants were subjected to Western blot analyses.

Antibodies. For immunofluorescence analysis, chicken anti-NP polyclonal antibody (19) (1:250), guinea pig anti-VP30 antibody (16) (1:250), and rabbit anti-VP30 antibody (16) (1:250) were used. The corresponding secondary antibodies used were goat anti-guinea pig Alexa Fluor 488 (Thermo Fisher Scientific) (1:500), goat anti-rabbit Alexa Fluor 488 (Thermo Fisher Scientific) (1:500), and donkey anti-chicken IRDye 680RD (Li-Cor) (1:500). For Western blot analysis, chicken anti-NP polyclonal antibody (19) (1:500), a monoclonal mouse anti-VP40 antibody (48) (1:500), a guinea pig anti-VP30 antibody (16) (1:500), a rabbit anti-pSer29 antibody (20) (1:100), a rabbit anti-SRPK1 antibody (Abcam) (1:250), and a mouse anti-alpha-tubulin antibody (Abcam) (1:500) were used. The corresponding secondary antibodies were donkey anti-chicken IRDye 680RD (Li-Cor) (1:500), donkey anti-chicken IRDye 800CW (Li-Cor) (1:500), donkey anti-guinea pig IRDye 800CW (Li-Cor) (1:500), goat anti-rabbit IRDye 680RD (Li-Cor) (1:500),

donkey anti-rabbit IRDye 680RD (Li-Cor) (1:500), swine polyclonal anti-rabbit immunoglobulin/horseradish peroxidase (HRP) (Dako) (1:500), donkey anti-rabbit IRDye 800CW (Li-Cor) (1:500), donkey anti-mouse IRDye 680RD (Li-Cor) (1:500), and goat anti-mouse IRDye 800CW (Li-Cor) (1:500).

SDS-PAGE and Western blot analysis. SDS-PAGE and Western blot analyses were performed as described previously (16, 49). Visualization of the signals was performed with Image Lab software for HRP-conjugated secondary antibodies or the Li-Cor Odyssey imaging system for fluorescently labeled secondary antibodies, as indicated above in the section on antibodies. The intensity of the obtained signals was analyzed by using the Fiji software package (v.1.52e) (50).

EBOV-specific minigenome assay. An EBOV-specific minigenome assay was performed as described previously (51). Briefly, the plasmids for the minigenome assay (125 ng of pCAGGS-NP, 125 ng of pCAGGS-VP35, 100 ng of pCAGGS-VP30, and 1,000 ng of pCAGGS-L, with 250 ng of a EBOV-specific minigenome carrying the *Renilla* luciferase reporter gene [3E5E-luc], 250 ng of pCAGGS-T7 polymerase, and 100 ng of the pCAGGS vector carrying the firefly luciferase reporter gene for normalization) were transfected into HEK293 cells seeded in 6-well plates. Reporter activity was measured at 48 h p.t. Optionally, the cells were treated with either 0.05% DMSO (control), 25 nM OA, or a mixture of 30 μM SRPIN340 and 25 nM OA for 18 h. At 48 h p.t., cells were lysed, and reporter gene activity was monitored by a luciferase assay (PJK, Germany).

EBOV-specific trVLP assay. For analysis of transcription/replication activity, an EBOV transcription- and replication-competent virus-like particle (trVLP) assay was performed as described previously (27, 52), with modifications. Briefly, HEK293 cells were seeded in a 6-well plate. Each well was transfected with plasmids encoding all EBOV structural proteins (125 ng of pCAGGS-NP, 125 ng of pCAGGS-VP35, 250 ng of pCAGGS-VP40, 250 ng of pCAGGS-GP, 100 ng of pCAGGS-VP30, 60 ng of pCAGGS-VP24, and 1,000 ng of pCAGGS-L), 250 ng of an EBOV-specific minigenome, 250 ng of pCAGGS-T7 polymerase, and 100 ng of the pCAGGS vector carrying the firefly luciferase reporter gene for normalization. Culture supernatants from three wells were collected at 72 h p.t., and released trVLPs were purified via ultracentrifugation through a 20% sucrose cushion. Optionally, an aliquot of trVLPs was subjected to a proteinase K digestion assay as described previously (53). The producer cells were lysed at 72 h p.t., and the indicator cells were lysed at 48 h p.i.; subsequently, a luciferase reporter assay (PJK, Germany) was performed.

Cell viability assay. To evaluate cell viability, the WST-1 cell proliferation assay system (TaKaRa) was used according to the manufacturer's recommendations. HEK293 cells (8×10^3 cells per well) or Huh-7 cells (2×10^3 cells per well) were seeded into 96-well microplates and incubated for 24 h at 37°C with 5% CO_2. The medium was replaced with fresh medium with either DMSO or various concentrations of SRPIN340 and incubated at 37°C under 5% CO_2. After 48 h of treatment, the medium was mixed with 10% WST-1 reagent, and the absorbance was measured using an Autobio PHOmo microplate reader (measurement wavelength, 450 nm; reference wavelength, 600 nm).

Rescue of recombinant EBOV. The recombinant EBOV (rEBOV^{wt}) used in this study was based on EBOV Zaire (strain Mayinga; GenBank accession number AF272001). Cloning and rescue of full-length EBOV were performed as described previously (54), with modifications. Briefly, 1,000 ng of full-length EBOV cDNA (based on pAMP rg ZEBOV, kindly provided by G. Neumann) and helper plasmids (125 ng pCAGGS-NP, 125 ng pCAGGS-VP35, 1,000 ng pCAGGS-L, 100 ng pCAGGS-VP30, and 250 ng pCAGGS-T7) were transfected into Huh-7 cells. The cell supernatants were transferred to fresh Huh-7 cells at 7 days p.t. Once the cells showed cytopathic effect (CPE), at approximately 7 to 10 days p.i., supernatants were collected and transferred to fresh Vero E6 cells (p2). The supernatants of p2 cells that showed CPE formation were harvested, aliquoted, and stored at −80°C for use in all further experiments. In order to verify the sequence of recombinant viruses, viral RNA was extracted from supernatants using a QIAamp viral RNA minikit (Qiagen) according to the manufacturer's instructions. Reverse transcription (RT) with ensuing PCR steps was performed using a Transcriptor one-step RT-PCR kit (Roche) with EBOV-specific primers. The resulting cDNA was sequenced. All work with infectious viruses was performed in the biosafety level 4 (BSL-4) facility at Philipps-Universität Marburg according to national laws.

EBOV infection. Growth kinetics of recombinant EBOV were determined in HEK293 or Huh-7 cells seeded into a 12-well plate at a multiplicity of infection (MOI) of 0.1 or 0.01. The inoculum was removed after 1 h, and cells were cultivated in DMEM containing 3% fetal calf serum (FCS), PS, and Q at 37°C under 5% CO_2. To analyze the effect of ectopically expressed SRPK1, cells were transfected with either 500 ng of pCAGGS-SRPK1 or an empty vector 12 h prior to infection. Aliquots of the cell supernatants were collected and stored at −80°C until use.

$TCID_{50}$ analysis. Virus titers were determined by a 50% tissue culture infectious dose ($TCID_{50}$) assay in Vero E6 cells as described previously (30).

Immunofluorescence confocal laser scanning microscopy. Immunofluorescence analysis was performed as described previously (55, 56). Microscopic images were acquired with a Leica SP5 confocal laser scanning microscope using a 63× oil objective (Leica Microsystems). Cells were grown on glass coverslips and fixed with 4% paraformaldehyde at 24 h p.t. or p.i. Optionally, nucleus staining was achieved by using DAPI (4′,6-diamidino-2-phenylindole). For quantification of the colocalization between VP30 and SRPK1, Pearson's correlation coefficient was calculated by using the Coloc2 plug-in (https://imagej.net/Coloc_2) for Fiji (v.1.52e) (50).

Electron microscopy analysis. We performed electron microscopy analyses of virus particles purified from the supernatants of HEK293 cells infected with either recVP30^{wt}, recVP30^{29S}, or recVP30^{26A29S}. Virions were adsorbed on finder grids and subsequently negatively stained with 2% phosphotungstic acid. Next, these grids were analyzed by using a JEM1400 transmission electron microscope.

Statistical analysis. The presented mean values and standard deviations (SD) are derived from at least three independent experiments. Statistical analysis was performed by using SPSS16.0 or GraphPad

Prism (version 7.03). Normally distributed samples were analyzed by a *t* test or one-way analysis of variance (ANOVA), and the other samples were analyzed by a nonparametric test. Statistically significant differences are indicated with asterisks in the figures (*, $P < 0.05$; **, $P < 0.01$; ***, $P < 0.001$; ****, $P < 0.0001$).

SUPPLEMENTAL MATERIAL

Supplemental material is available online only.

FIG S1, TIFF file, 0.3 MB.

FIG S2, TIFF file, 0.1 MB.

FIG S3, TIFF file, 0.3 MB.

FIG S4, TIFF file, 0.2 MB.

FIG S5, TIFF file, 0.2 MB.

TABLE S1, PDF file, 0.1 MB.

ACKNOWLEDGMENTS

We thank Dirk Becker, Sonja Heck, Astrid Herwig, Katharina Kowalski, and Cornelius Rohde for technical support. BSL-4 work would not have been possible without the supervision of Markus Eickmann, Olga Dolnik, and Thomas Strecker and technical support by Michael Schmidt and Gotthard Ludwig. We thank Jakob Nilsson for critical reading of the manuscript and very helpful discussions.

The work was supported by overseas research fellowships of the Uehara Memorial Foundation, the Japan Society for the Promotion of Science (JSPS) (grant numbers 18J01631 and 19K16666), the MSD Life Science Foundation (ID-022), the Japan Research Foundation for Clinical Pharmacology, and the Terumo Life Science Foundation (19-III455) (to Yuki Takamatsu); by the Deutsche Forschungsgemeinschaft (DFG) through SFB 1021 projects A02 and B03 (to Larissa Kolesnikova, Nadine Biedenkopf, and Stephan Becker); by the German Center for Infection Research, Emerging Infections (to Verena Krähling, Nadine Biedenkopf, and Stephan Becker); and by the AMED Research Program on Emerging and Reemerging Infectious Diseases, the AMED Japanese Initiative for Progress of Research on Infectious Disease for Global Epidemic, JSPS Core-to-Core Program A, the Advanced Research Networks, a grant for the Joint Research Project of the Institute of Medical Science, University of Tokyo, the Joint Usage/Research Center Program of the Institute for Frontier Life and Medical Sciences, Kyoto University, the Daiichi Sankyo Foundation of Life Science, and the Takeda Science Foundation (to Takeshi Noda).

Yuki Takamatsu and Stephan Becker conceived the project and designed the experiments. Verena Krähling, Larissa Kolesnikova, Clemens Lier, Takeshi Noda, and Stefan Baumeister supported experiments by providing materials and technical troubleshooting. Yuki Takamatsu, Verena Krähling, and Larissa Kolesnikova performed experiments, and analyses were performed by Yuki Takamatsu, Sandro Halwe, Nadine Biedenkopf, and Stephan Becker. The manuscript was written by Yuki Takamatsu, Verena Krähling, Larissa Kolesnikova, Sandro Halwe, Stefan Baumeister, Takeshi Noda, Nadine Biedenkopf, and Stephan Becker.

We declare no competing interests.

REFERENCES

1. Shi Y. 2009. Serine/threonine phosphatases: mechanism through structure. Cell 139:468–484. https://doi.org/10.1016/j.cell.2009.10.006.
2. Lubbers ER, Mohler PJ. 2016. Roles and regulation of protein phosphatase 2A (PP2A) in the heart. J Mol Cell Cardiol 101:127–133. https://doi.org/10.1016/j.yjmcc.2016.11.003.
3. Berndt N, Karim RM, Schonbrunn E. 2017. Advances of small molecule targeting of kinases. Curr Opin Chem Biol 39:126–132. https://doi.org/10.1016/j.cbpa.2017.06.015.
4. Jakubiec A, Jupin I. 2007. Regulation of positive-strand RNA virus replication: the emerging role of phosphorylation. Virus Res 129:73–79. https://doi.org/10.1016/j.virusres.2007.07.012.
5. Hemonnot B, Cartier C, Gay B, Rebuffat S, Bardy M, Devaux C, Boyer V, Briant L. 2004. The host cell MAP kinase ERK-2 regulates viral assembly and release by phosphorylating the p6gag protein of HIV-1. J Biol Chem 279:32426–32434. https://doi.org/10.1074/jbc.M313137200.
6. Das SC, Pattnaik AK. 2004. Phosphorylation of vesicular stomatitis virus phosphoprotein P is indispensable for virus growth. J Virol 78:6420–6430. https://doi.org/10.1128/JVI.78.12.6420-6430.2004.
7. Law LM, Everitt JC, Beatch MD, Holmes CF, Hobman TC. 2003. Phosphorylation of rubella virus capsid regulates its RNA binding activity and virus replication. J Virol 77:1764–1771. https://doi.org/10.1128/jvi.77.3.1764-1771.2003.
8. Ross-Thriepland D, Mankouri J, Harris M. 2015. Serine phosphorylation of the hepatitis C virus NS5A protein controls the establishment of replication complexes. J Virol 89:3123–3135. https://doi.org/10.1128/JVI.02995-14.

9. Eichwald C, Vascotto F, Fabbretti E, Burrone OR. 2002. Rotavirus NSP5: mapping phosphorylation sites and kinase activation and viroplasm localization domains. J Virol 76:3461–3470. https://doi.org/10.1128/jvi.76.7.3461-3470.2002.
10. Modrof J, Muhlberger E, Klenk HD, Becker S. 2002. Phosphorylation of VP30 impairs Ebola virus transcription. J Biol Chem 277:33099–33104. https://doi.org/10.1074/jbc.M203775200.
11. Keshtkar-Jahromi M, Martins KAO, Cardile AP, Reisler RB, Christopher GW, Bavari S. 2018. Treatment-focused Ebola trials, supportive care and future of filovirus care. Expert Rev Anti Infect Ther 16:67–76. https://doi.org/10.1080/14787210.2018.1413937.
12. Ma-Lauer Y, Lei J, Hilgenfeld R, von Brunn A. 2012. Virus-host interactomes—antiviral drug discovery. Curr Opin Virol 2:614–621. https://doi.org/10.1016/j.coviro.2012.09.003.
13. Saeed MF, Kolokoltsov AA, Albrecht T, Davey RA. 2010. Cellular entry of Ebola virus involves uptake by a macropinocytosis-like mechanism and subsequent trafficking through early and late endosomes. PLoS Pathog 6:e1001110. https://doi.org/10.1371/journal.ppat.1001110.
14. Muhlberger E, Weik M, Volchkov VE, Klenk HD, Becker S. 1999. Comparison of the transcription and replication strategies of Marburg virus and Ebola virus by using artificial replication systems. J Virol 73:2333–2342. https://doi.org/10.1128/JVI.73.3.2333-2342.1999.
15. Elliott LH, Kiley MP, McCormick JB. 1985. Descriptive analysis of Ebola virus proteins. Virology 147:169–176. https://doi.org/10.1016/0042-6822(85)90236-3.
16. Biedenkopf N, Hartlieb B, Hoenen T, Becker S. 2013. Phosphorylation of Ebola virus VP30 influences the composition of the viral nucleocapsid complex: impact on viral transcription and replication. J Biol Chem 288:11165–11174. https://doi.org/10.1074/jbc.M113.461285.
17. Biedenkopf N, Schlereth J, Grunweller A, Becker S, Hartmann RK. 2016. RNA binding of Ebola virus VP30 is essential for activating viral transcription. J Virol 90:7481–7496. https://doi.org/10.1128/JVI.00271-16.
18. Ilinykh PA, Tigabu B, Ivanov A, Ammosova T, Obukhov Y, Garron T, Kumari N, Kovalskyy D, Platonov MO, Naumchik VS, Freiberg AN, Nekhai S, Bukreyev A. 2014. Role of protein phosphatase 1 in dephosphorylation of Ebola virus VP30 protein and its targeting for the inhibition of viral transcription. J Biol Chem 289:22723–22738. https://doi.org/10.1074/jbc.M114.575050.
19. Biedenkopf N, Lier C, Becker S. 2016. Dynamic phosphorylation of VP30 is essential for Ebola virus life cycle. J Virol 90:4914–4925. https://doi.org/10.1128/JVI.03257-15.
20. Lier C, Becker S, Biedenkopf N. 2017. Dynamic phosphorylation of Ebola virus VP30 in NP-induced inclusion bodies. Virology 512:39–47. https://doi.org/10.1016/j.virol.2017.09.006.
21. Kirchdoerfer RN, Moyer CL, Abelson DM, Saphire EO. 2016. The Ebola virus VP30-NP interaction is a regulator of viral RNA synthesis. PLoS Pathog 12:e1005937. https://doi.org/10.1371/journal.ppat.1005937.
22. Kruse T, Biedenkopf N, Hertz EPT, Dietzel E, Stalmann G, Lopez-Mendez B, Davey NE, Nilsson J, Becker S. 2018. The Ebola virus nucleoprotein recruits the host PP2A-B56 phosphatase to activate transcriptional support activity of VP30. Mol Cell 69:136–145. https://doi.org/10.1016/j.molcel.2017.11.034.
23. Okamoto K, Endo Y, Inoue S, Nabeshima T, Nga PT, Guillermo PH, Yu F, Loan DP, Trang BM, Natividad FF, Hasebe F, Morita K. 2010. Development of a rapid and comprehensive proteomics-based arboviruses detection system. J Virol Methods 167:31–36. https://doi.org/10.1016/j.jviromet.2010.03.006.
24. Okuda S, Watanabe Y, Moriya Y, Kawano S, Yamamoto T, Matsumoto M, Takami T, Kobayashi D, Araki N, Yoshizawa AC, Tabata T, Sugiyama N, Goto S, Ishihama Y. 2017. jPOSTrepo: an international standard data repository for proteomes. Nucleic Acids Res 45:D1107–D1111. https://doi.org/10.1093/nar/gkw1080.
25. Fukuhara T, Hosoya T, Shimizu S, Sumi K, Oshiro T, Yoshinaka Y, Suzuki M, Yamamoto N, Herzenberg LA, Hagiwara M. 2006. Utilization of host SR protein kinases and RNA-splicing machinery during viral replication. Proc Natl Acad Sci U S A 103:11329–11333. https://doi.org/10.1073/pnas.0604616103.
26. Karakama Y, Sakamoto N, Itsui Y, Nakagawa M, Tasaka-Fujita M, Nishimura-Sakurai Y, Kakinuma S, Oooka M, Azuma S, Tsuchiya K, Onogi H, Hagiwara M, Watanabe M. 2010. Inhibition of hepatitis C virus replication by a specific inhibitor of serine-arginine-rich protein kinase. Antimicrob Agents Chemother 54:3179–3186. https://doi.org/10.1128/AAC.00113-10.
27. Hoenen T, Groseth A, Kolesnikova L, Theriault S, Ebihara H, Hartlieb B, Bamberg S, Feldmann H, Stroher U, Becker S. 2006. Infection of naive target cells with virus-like particles: implications for the function of Ebola virus VP24. J Virol 80:7260–7264. https://doi.org/10.1128/JVI.00051-06.
28. Hoenen T, Biedenkopf N, Zielecki F, Jung S, Groseth A, Feldmann H, Becker S. 2010. Oligomerization of Ebola virus VP40 is essential for particle morphogenesis and regulation of viral transcription. J Virol 84:7053–7063. https://doi.org/10.1128/JVI.00737-10.
29. Biedenkopf N, Hoenen T. 2017. Modeling the ebolavirus life cycle with transcription and replication-competent viruslike particle assays. Methods Mol Biol 1628:119–131. https://doi.org/10.1007/978-1-4939-7116-9_9.
30. Krähling V, Dolnik O, Kolesnikova L, Schmidt-Chanasit J, Jordan I, Sandig V, Günther S, Becker S. 2010. Establishment of fruit bat cells (Rousettus aegyptiacus) as a model system for the investigation of filoviral infection. PLoS Negl Trop Dis 4:e802. https://doi.org/10.1371/journal.pntd.0000802.
31. Fisher TL, Blenis J. 1996. Evidence for two catalytically active kinase domains in pp90rsk. Mol Cell Biol 16:1212–1219. https://doi.org/10.1128/mcb.16.3.1212.
32. Kang JH, Jiang Y, Toita R, Oishi J, Kawamura K, Han A, Mori T, Niidome T, Ishida M, Tatematsu K, Tanizawa K, Katayama Y. 2007. Phosphorylation of Rho-associated kinase (Rho-kinase/ROCK/ROK) substrates by protein kinases A and C. Biochimie 89:39–47. https://doi.org/10.1016/j.biochi.2006.08.003.
33. Martinez MJ, Biedenkopf N, Volchkova V, Hartlieb B, Alazard-Dany N, Reynard O, Becker S, Volchkov V. 2008. Role of Ebola virus VP30 in transcription reinitiation. J Virol 82:12569–12573. https://doi.org/10.1128/JVI.01395-08.
34. Czubaty A, Piekiełko-Witkowska A. 2017. Protein kinases that phosphorylate splicing factors: roles in cancer development, progression and possible therapeutic options. Int J Biochem Cell Biol 91:102–115. https://doi.org/10.1016/j.biocel.2017.05.024.
35. Sciabica KS, Dai QJ, Sandri-Goldin RM. 2003. ICP27 interacts with SRPK1 to mediate HSV splicing inhibition by altering SR protein phosphorylation. EMBO J 22:1608–1619. https://doi.org/10.1093/emboj/cdg166.
36. Bell I, Martin A, Roberts S. 2007. The E1^E4 protein of human papillomavirus interacts with the serine-arginine-specific protein kinase SRPK1. J Virol 81:5437–5448. https://doi.org/10.1128/JVI.02609-06.
37. Prescott EL, Brimacombe CL, Hartley M, Bell I, Graham S, Roberts S. 2014. Human papillomavirus type 1 E1^E4 protein is a potent inhibitor of the serine-arginine (SR) protein kinase SRPK1 and inhibits phosphorylation of host SR proteins and of the viral transcription and replication regulator E2. J Virol 88:12599–12611. https://doi.org/10.1128/JVI.02029-14.
38. Zheng Y, Fu XD, Ou J-HJ. 2005. Suppression of hepatitis B virus replication by SRPK1 and SRPK2 via a pathway independent of the phosphorylation of the viral core protein. Virology 342:150–158. https://doi.org/10.1016/j.virol.2005.07.030.
39. Daub H, Blencke S, Habenberger P, Kurtenbach A, Dennenmoser J, Wissing J, Ullrich A, Cotten M. 2002. Identification of SRPK1 and SRPK2 as the major cellular protein kinases phosphorylating hepatitis B virus core protein. J Virol 76:8124–8137. https://doi.org/10.1128/jvi.76.16.8124-8137.2002.
40. Weik M, Modrof J, Klenk HD, Becker S, Muhlberger E. 2002. Ebola virus VP30-mediated transcription is regulated by RNA secondary structure formation. J Virol 76:8532–8539. https://doi.org/10.1128/jvi.76.17.8532-8539.2002.
41. Xu W, Luthra P, Wu C, Batra J, Leung DW, Basler CF, Amarasinghe GK. 2017. Ebola virus VP30 and nucleoprotein interactions modulate viral RNA synthesis. Nat Commun 8:15576. https://doi.org/10.1038/ncomms15576.
42. Schlereth J, Grunweller A, Biedenkopf N, Becker S, Hartmann RK. 2016. RNA binding specificity of Ebola virus transcription factor VP30. RNA Biol 13:783–798. https://doi.org/10.1080/15476286.2016.1194160.
43. Becker S, Rinne C, Hofsass U, Klenk HD, Muhlberger E. 1998. Interactions of Marburg virus nucleocapsid proteins. Virology 249:406–417. https://doi.org/10.1006/viro.1998.9328.
44. Takamatsu Y, Kolesnikova L, Becker S. 2018. Ebola virus proteins NP, VP35, and VP24 are essential and sufficient to mediate nucleocapsid transport. Proc Natl Acad Sci U S A 115:1075–1080. https://doi.org/10.1073/pnas.1712263115.
45. Hellman U, Wernstedt C, Gonez J, Heldin CH. 1995. Improvement of an "in-gel" digestion procedure for the micropreparation of internal protein fragments for amino acid sequencing. Anal Biochem 224:451–455. https://doi.org/10.1006/abio.1995.1070.
46. Zadmard R, Kraft A, Schrader T, Linne U. 2004. Relative binding affinities

of molecular capsules investigated by ESI-mass spectrometry. Chemistry 10:4233–4239. https://doi.org/10.1002/chem.200400034.
47. Perkins DN, Pappin DJ, Creasy DM, Cottrell JS. 1999. Probability-based protein identification by searching sequence databases using mass spectrometry data. Electrophoresis 20:3551–3567. https://doi.org/10.1002/(SICI)1522-2683(19991201)20:18<3551::AID-ELPS3551>3.0.CO;2-2.
48. Hoenen T, Volchkov V, Kolesnikova L, Mittler E, Timmins J, Ottmann M, Reynard O, Becker S, Weissenhorn W. 2005. VP40 octamers are essential for Ebola virus replication. J Virol 79:1898–1905. https://doi.org/10.1128/JVI.79.3.1898-1905.2005.
49. Kolesnikova L, Berghofer B, Bamberg S, Becker S. 2004. Multivesicular bodies as a platform for formation of the Marburg virus envelope. J Virol 78:12277–12287. https://doi.org/10.1128/JVI.78.22.12277-12287.2004.
50. Schindelin J, Arganda-Carreras I, Frise E, Kaynig V, Longair M, Pietzsch T, Preibisch S, Rueden C, Saalfeld S, Schmid B, Tinevez JY, White DJ, Hartenstein V, Eliceiri K, Tomancak P, Cardona A. 2012. Fiji: an open-source platform for biological-image analysis. Nat Methods 9:676–682. https://doi.org/10.1038/nmeth.2019.
51. Hoenen T, Jung S, Herwig A, Groseth A, Becker S. 2010. Both matrix proteins of Ebola virus contribute to the regulation of viral genome replication and transcription. Virology 403:56–66. https://doi.org/10.1016/j.virol.2010.04.002.
52. Hoenen T, Groseth A, de Kok-Mercado F, Kuhn JH, Wahl-Jensen V. 2011. Minigenomes, transcription and replication competent virus-like particles and beyond: reverse genetics systems for filoviruses and other negative stranded hemorrhagic fever viruses. Antiviral Res 91:195–208. https://doi.org/10.1016/j.antiviral.2011.06.003.
53. Wenigenrath J, Kolesnikova L, Hoenen T, Mittler E, Becker S. 2010. Establishment and application of an infectious virus-like particle system for Marburg virus. J Gen Virol 91:1325–1334. https://doi.org/10.1099/vir.0.018226-0.
54. Groseth A, Marzi A, Hoenen T, Herwig A, Gardner D, Becker S, Ebihara H, Feldmann H. 2012. The Ebola virus glycoprotein contributes to but is not sufficient for virulence in vivo. PLoS Pathog 8:e1002847. https://doi.org/10.1371/journal.ppat.1002847.
55. Dolnik O, Kolesnikova L, Stevermann L, Becker S. 2010. Tsg101 is recruited by a late domain of the nucleocapsid protein to support budding of Marburg virus-like particles. J Virol 84:7847–7856. https://doi.org/10.1128/JVI.00476-10.
56. Kolesnikova L, Mittler E, Schudt G, Shams-Eldin H, Becker S. 2012. Phosphorylation of Marburg virus matrix protein VP40 triggers assembly of nucleocapsids with the viral envelope at the plasma membrane. Cell Microbiol 14:182–197. https://doi.org/10.1111/j.1462-5822.2011.01709.x.